Mechanism of proton/substrate coupling in the heptahelical lysosomal transporter cystinosin

Raquel Ruivo[a,b,1], Gian Carlo Bellenchi[c], Xiong Chen[a], Giovanni Zifarelli[d], Corinne Sagné[a], Cécile Debacker[a], Michael Pusch[d], Stéphane Supplisson[e,f,g], and Bruno Gasnier[a,2]

[a]Université Paris Descartes, Sorbonne Paris Cité, Centre National de la Recherche Scientifique, Unité Mixte de Recherche 8192, Centre Universitaire des Saints-Pères, 45 rue des Saints-Pères, F-75006 Paris, France; [b]Graduate School ED 419, Université Paris-Sud 11, Hôpital Bicêtre, Bâtiment Grégory Pincus, 80 rue du Général Leclerc, F-94276 Le Kremlin Bicêtre, France; [c]Istituto di Genetica e Biofisica, Consiglio Nazionale delle Ricerche, Via Pietro Castellino 111, I-80131 Naples, Italy; [d]Istituto di Biofisica, Consiglio Nazionale delle Ricerche, Via De Marini, 6, I-16149 Genoa, Italy; [e]Institut de Biologie de l'Ecole Normale Supérieure, F-75005 Paris, France; [f]Centre National de la Recherche Scientifique, Unité Mixte de Recherche 8197, F-75005 Paris, France; and [g]Institut National de la Santé et de la Recherche Médicale U1024, F-75005 Paris, France

Edited by Christopher Miller, Howard Hughes Medical Institute, Brandeis University, Waltham, MA, and approved November 30, 2011 (received for review September 22, 2011)

Secondary active transporters use electrochemical gradients provided by primary ion pumps to translocate metabolites or drugs "uphill" across membranes. Here we report the ion-coupling mechanism of cystinosin, an unusual eukaryotic, proton-driven transporter distantly related to the proton pump bacteriorhodopsin. In humans, cystinosin exports the proteolysis-derived dimeric amino acid cystine from lysosomes and is impaired in cystinosis. Using voltage-dependence analysis of steady-state and transient currents elicited by cystine and neutralization-scanning mutagenesis of conserved protonatable residues, we show that cystine binding is coupled to protonation of a clinically relevant aspartate buried in the membrane. Deuterium isotope substitution experiments are consistent with an access of this aspartate from the lysosomal lumen through a deep proton channel. This aspartate lies in one of the two PQ-loop motifs shared by cystinosin with a set of eukaryotic membrane proteins of unknown function and is conserved in about half of them, thus suggesting that other PQ-loop proteins may translocate protons.

Life requires a busy traffic of ions and small molecules across plasma and intracellular membranes, which flows from primary active (ATP-, redox-, or light-driven) transporters to secondary active transporters and channels. While the first class of transport proteins creates the founding transmembrane gradients for this traffic, the second converts them to expand the repertoire of actively transported compounds, and the third dissipates them. Although these three classes of players have long been held as unrelated mechanistic entities, recent exceptional cases of transition between these classes, such as the coexistence of channels and secondary transporters for chloride within the ClC protein family (1, 2) or the conversion of the Na^+, K^+-ATPase to an open channel by a marine toxin (3), have unveiled similarities in the gating and ion-conduction properties of transporters and channels (4–8)—see ref. 9 for review.

The lysosomal cystine transporter cystinosin (10, 11) may offer a unique starting point to explore transitions between primary and secondary transporters because of its distant homology with microbial rhodopsins (12). The latter are a group of seven-helix membrane proteins that use retinal, a covalently linked prosthetic group, to absorb light energy for ion pumping or phototaxis function. Although initially discovered in archaea, including the well characterized *Halobacterium salinarum* proton pump bacteriorhodopsin (13), homologues have since been found in bacteria, fungi, and algae (14–16). The sole homology with mammalian proteins documented thus far is their distant relationship with the cystinosin protein family (12). The evolutionary relationship, if any, of microbial (type I) rhodopsins with animal (type II) opsins remains unclear (14).

Cystinosin has been identified as the causative gene product of cystinosis (10), a rare, autosomal recessive human disease (OMIM 21980) caused by defective efflux of cystine from lysosomes (17, 18). It starts with growth failure and proximal renal tubulopathy in the first year of age and evolves into terminal kidney failure and multisystemic damages if left untreated. Juvenile and nonnephropathic, adult forms have also been described (19, 20). Cystinosin orthologues are only found in eukaryotes (10, 21). Human cystinosin possesses seven putative transmembrane α-helices (TMs), with a large (120 amino acids), glycosylated N-terminal domain facing the lysosomal lumen and a short cytosolic C terminus containing a sorting motif responsible for its delivery to late endosomes and lysosomes (22). Another distinctive feature of the cystinosin sequence is the presence of a duplicated motif (InterPro database entry # IPR006603; http://www.ebi.ac.uk/interpro/), termed PQ-loop motif after the presence of a conserved proline-glutamine dipeptide (12, 23) (see blue stretches in Fig. 1). The functional significance of PQ loops remains unclear, the sole evidence being a contribution to lysosomal targeting without assignment, however, to specific residues (22).

In this study, we investigated the ion-coupling and transport mechanism of cystinosin using voltage-clamp analysis. We show that it cotransports protons and cystine, and that cystine binding is coupled to protonation of a clinically relevant, membrane-buried aspartate located in the second PQ loop. This aspartate undergoes reversible protonation upon cystine binding-unbinding, and it apparently receives its luminal proton through a deep access channel spanning approximately 65 percent of the membrane electric field. Our data suggest that PQ loops are core elements of the transport mechanism and that other PQ-loop proteins may translocate protons.

Results

Cystinosin Is a 1:1 H^+/cystine Symporter. To characterize the transport activity of human cystinosin (11), we expressed it in *Xenopus laevis* oocytes and recorded currents elicited by L-cystine under two-electrode voltage clamp. Deletion of the C-terminal lysosomal sorting motif (GYDQL) (22) misrouted EGFP-tagged cystinosin to the oocyte surface (Fig. 2*A* and Fig. S1). This effect was associated with induction of a robust inward current when 1 mM L-cystine was applied in extracellular acidic medium (Fig. 2 *A* and *B* and Table S1), a condition mimicking the natural environment in the lysosome (the extracellular medium in our assay

Author contributions: R.R., G.C.B., X.C., G.Z., M.P., S.S., and B.G. designed research; R.R., G.C.B., X.C., G.Z., C.S., C.D., S.S., and B.G. performed research; R.R., G.C.B., X.C., G.Z., C.S., M.P., S.S., and B.G. analyzed data; and B.G. wrote the paper.

The authors declare no conflict of interest.

This article is a PNAS Direct Submission.

[1]Present address: CIMAR/CIIMAR-Interdisciplinary Center of Marine and Environmental Research, University of Porto, Portugal.

[2]To whom correspondence should be addressed. E-mail: bruno.gasnier@parisdescartes.fr.

This article contains supporting information online at www.pnas.org/lookup/suppl/doi:10.1073/pnas.1115581109/-/DCSupplemental.

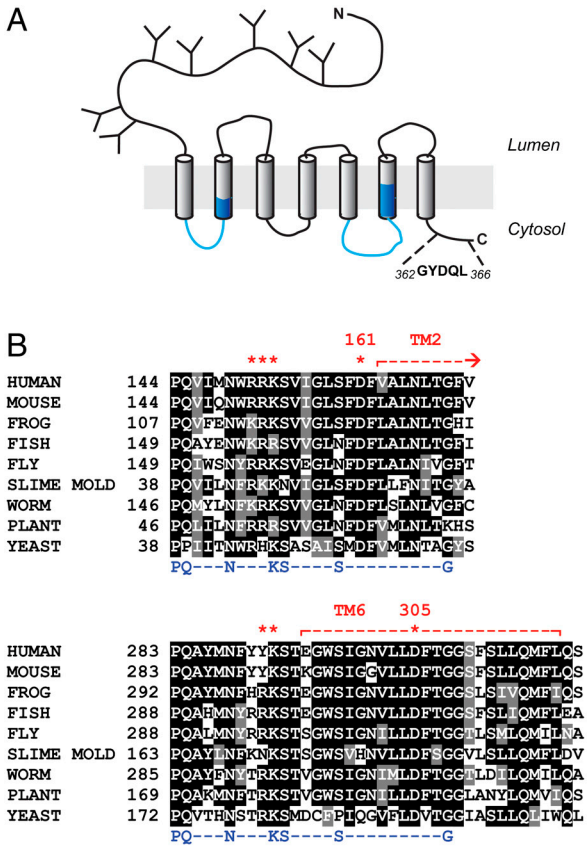

Fig. 1. Biochemical features of human cystinosin. (*A*) Putative topology. The sequence in the C terminus corresponds to the lysosomal sorting motif. PQ-loop motifs are highlighted in blue. (*B*) Multiple sequence alignment of cystinosin in the PQ-loop regions. The PQ-loop consensus sequence is indicated in blue. Protonatable residues included in the neutralization scan are labeled with red stars.

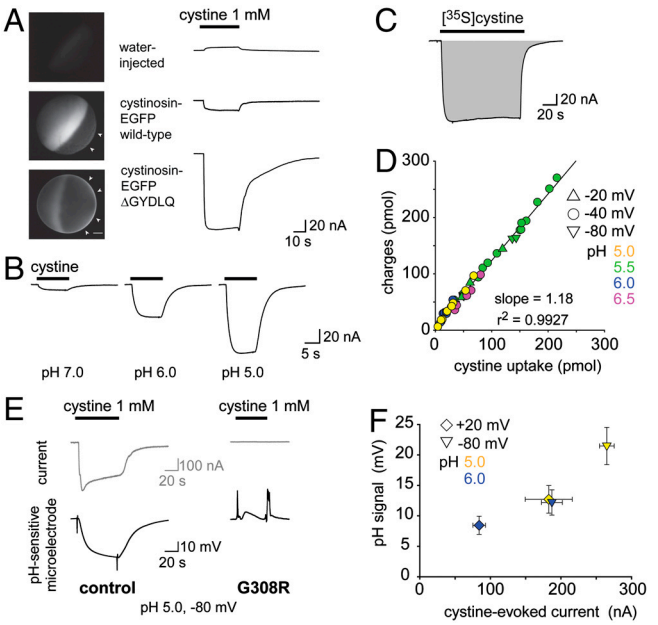

Fig. 2. Cystinosin is a 1:1 H^+/ cystine symporter. (*A*) mRNA-injected oocytes were analyzed by epifluorescence microscopy and by two-electrode voltage clamp. Expression of EGFP-tagged, wild-type human cystinosin induces a low level of fluorescence at the oocyte plasma membrane (second micrograph from top, arrowheads) and a small inward current upon application of 1 mM extracellular cystine at pH_{out} 5.0. Fluorescence at the plasma membrane and cystine-evoked current are dramatically increased after deletion of the lysosomal sorting motif GYDQL. The small outward current seen in water-injected oocytes is a mechanical artifact of the OpusXpress workstation, also observed when cystine-free buffer is applied. Scale bar, 0.2 mm. (*B*) An oocyte expressing human cystinosin-ΔGYDQL without EGFP tag was recorded at distinct pH values. (*C* and *D*) [^{35}S]cystine was applied to 45 cystinosin-ΔGYDQL oocytes under diverse voltage and pH_{out} conditions in two independent experiments. After recording, microelectrodes were removed and oocytes were counted by liquid scintillation. Time integral of cystine-evoked current (shaded area in *C*) is plotted in *D* as a function of [^{35}S]cystine uptake. (*E*) Cystinosin translocates protons. Recording with a pH-sensitive microelectrode in the vicinity of a clamped cystinosin-ΔGYDQL-EGFP oocyte shows that the cystine-evoked inward current is associated with extracellular alkalinization. Both responses were abolished by the loss-of-function pathogenic mutation G308R. (*F*) Cystine-evoked alkalinization is proportional to the inward current. Means ± s.e.m. of 7 oocytes.

being topologically equivalent to the lysosomal lumen). Some membrane transporters display an electrodiffusive conductance induced by, but uncoupled from, their transport activity (24–26). We thus tested whether the cystine-evoked current is tightly associated with cystine uptake by applying radiolabelled cystine to voltage-clamped oocytes. Scintillation counting of oocytes recorded at various extracellular pH values and membrane potentials showed that the time integral of the currents was proportional to the amount of accumulated [^{35}S]cystine, with a slope of 1.18 elementary charge per cystine molecule ($r^2 = 0.9927$, $n = 45$) (Fig. 2 *C* and *D*). Because cystine is zwitterionic at $3 < pH < 7.5$, this implies that it is cotransported with one monovalent cation or exchanged for one monovalent anion. Replacement of extracellular Na^+ with Li^+ or choline did not alter cystine-evoked currents (Fig. S2*A*). On the other hand, apposition of a H^+-selective microelectrode to voltage-clamped oocytes under lowered buffer concentration showed that cystinosin activity is associated with local extracellular alkalinization (Fig. 2*E*). The magnitude of the pH signal correlated with the steady-state current (Fig. 2*F*) and the introduction of a loss-of-function point mutation (G308R) causing infantile cystinosis (11, 27, 28) abolished both the current and extracellular alkalinization responses (Fig. 2*E* and Fig. S2*C*). We concluded from the above data that human cystinosin cotransports H^+ and cystine with a 1:1 stoichiometry. Other potential stoichiometries ($2H^+$,$1Cl^-$ cotransport; exchange of $2H^+$ against $1K^+$) were excluded by replacing extracellular Cl^- with gluconate or raising extracellular K^+ up to 100 mM (Fig. S2 *A* and *B*).

Substrate Selectivity. We next tested the ability of several amino acids (1 mM) to evoke currents in cystinosin-expressing oocytes. Although earlier studies suggested that some amino acids compete with cystine transport (11, 29), none of the canonical L-amino acids, including L-cysteine, induced current (Fig. S2 *D* and *E*), implying that they are not translocated. L-selenomethionine (1 mM) elicited a small inward current, whereas cystine analogues such as L-selenocystine and L-cystathionine induced robust currents (Fig. S2*F*), in agreement with earlier biochemical studies (29). These data indicate that cystinosin, unlike most lysosomal transporters (30), has narrow substrate selectivity.

pH and Voltage Dependence of the Steady-State Current. We next examined the dependence of the steady-state current on cystine concentration under diverse membrane potential (V_m) and extracellular pH (pH_{out}) conditions, by applying voltage jumps in the presence of increasing concentrations of L-cystine (Fig. 3 *A* and *B*). Michaelis constant (K_m), Hill number and maximal current (I_{max}) values derived from the saturation curves are shown in Fig. 3 *C*–*E*, respectively. The transport activity followed Michaelis–Menten kinetics over the voltage and pH ranges tested (Fig. 3 *B* and *D*). Intriguingly, the voltage dependence of the K_m for cystine was strongly affected by pH_{out}. Whereas K_m was minimal (75 μM) and independent of V_m at pH 5.0, it increased

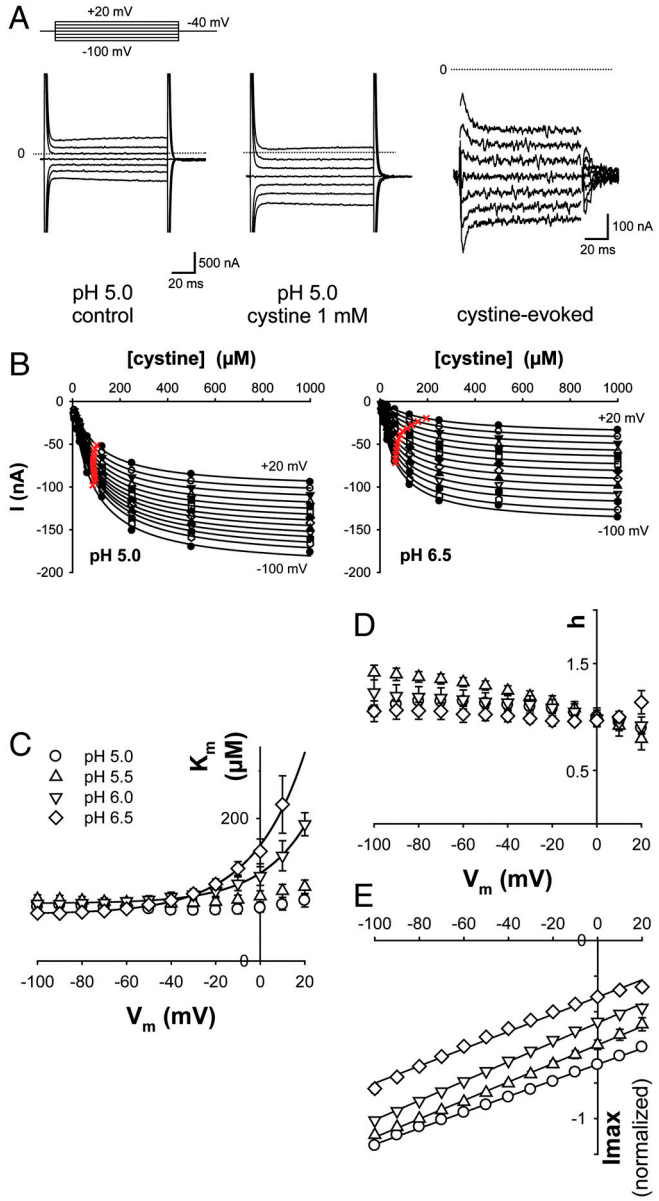

Fig. 3. Voltage and pH dependence of steady-state kinetics. (*A*) Cystinosin-ΔGYDQL-EGFP oocytes were held at -40 mV and stepped to various potentials before and during cystine application. Raw OpusXpress traces are shown in the left and central panels. Subtracting these traces reveals the cystine-induced component (*Right*). The position of zero current is shown by the dotted lines. (*B*) Voltage steps were repeated for 8 cystine concentrations (8 μM-1 mM) at several pH values. Cystine-induced steady-state current follows Michaelis–Menten saturation kinetics. Half-maximal current is marked with a red cross. (*C–E*) K_m for cystine, Hill number (h) and I_{max} derived from the saturation curves are plotted as a function of membrane potential (V_m) at 4 pH_{out} values (4 to 9 oocytes). Because I_{max} depends on the amount of cystinosin present at the plasma membrane, data in *E* were normalized to the I_{max} value obtained at pH 5.5 and −80 mV. The voltage dependence of K_m strongly depends on pH_{out}, whereas I_{max} varies linearly with V_m in a pH_{out}-independent manner. After multiplication by the mean I_{max} value at pH_{out} 5.5 and −80 mV (−169 ± 24 nA), a slope of 0.84 ± 0.09 nA·mV^{-1} is obtained regardless of pH_{out}.

exponentially with V_m for pH values ≥6.0 (Fig. 3*C* and Fig. S3). In contrast, the maximal current (I_{max}) displayed the same linear dependence on V_m regardless of pH_{out} (Fig. 3*E*).

The most parsimonious hypothesis accounting for the peculiar voltage and pH dependence of K_m is to postulate (*i*) that cystine binding is favored by protonation of a residue accessible to the extracellular compartment (equivalent to the lysosomal lumen) and (*ii*) that this residue is buried in the membrane, thereby sensing a local pH influenced by the membrane potential. At pH_{out} 5.0, this residue would be fully protonated over the voltage range tested (−100 to +20 mV), thus ensuring maximal affinity for cystine. At pH ≥ 6.0 and $V_m > 0$ mV, it would be partly deprotonated, resulting in lower cystine affinity; however, membrane hyperpolarization would rescue full protonation and high-affinity cystine binding by attracting extracellular H^+ around the protonatable residue. Conversely, membrane depolarization should alkalinize the residue microenvironment and, therefore, decrease cystine binding. In this model, the relationship between the microenvironmental pH around the protonatable residue and the bulk pH_{out} follows a Woodhull equation (31), thus explaining the exponential voltage dependence of K_m (see *SI Text*).

Cystine-Bound Cystinosin Shows Capacitive Charge Movements. As mutational analysis of steady-state currents was inconclusive, we used transient kinetic analysis to test our working model. We reasoned that protonation and deprotonation from/to the extracellular compartment of a residue buried in the electric field might elicit detectable and opposite charge movement. Because fast application of cystine proved difficult, we used a different approach (32, 33) consisting of applying voltage jumps before and after equilibrating oocytes with a saturating concentration of cystine (1 mM). After raw trace subtraction, cystine-dependent responses might reveal transient currents associated with shifts of the cystinosin protonation equilibrium towards protonated or nonprotonated states according to our model.

These experiments were performed at pH_{out} 7.5 to minimize transport activity. Fig. 4*A* shows the outcome of such an experiment for a cystinosin-ΔGYDQL-EGFP oocyte. At this slightly alkaline pH, the steady-state current evoked by cystine was almost absent. Depolarizing and subsequent repolarizing steps induced robust outward and inward cystine-dependent transient currents, respectively, indicating that the voltage jumps trigger charge movements in the cystine-bound state of cystinosin. Hyperpolarizing jumps had opposite effects, yet with a much lower magnitude, a feature indicating that the electrogenic transition challenged by the voltage jumps is almost fully shifted to one state at the holding potential (−40 mV).

The capacitive origin of the transient currents carried by cystine-bound cystinosin was supported by the fact that identical time integrals (ΔQ) of the transient currents were obtained upon stepping from (ON steps) and back to (OFF steps) the holding potential (Fig. 4*B*). This voltage dependence was well fitted by a Boltzmann function:

$$Q(V) = Q_{max}/(1 + e^{-z\,\delta^*(V_m - V_{0.5})F/RT}) \quad [1]$$

where z is the fraction of elementary charge moving in each cystinosin molecule, δ^* the fraction of the electric field across which the charge moves, Q_{max} the maximal amount of movable charges for the whole population of cystinosin molecules and $V_{0.5}$ the membrane potential at which charge movement is half-completed (32). Mean Q_{max}, $V_{0.5}$, and $z\delta^*$ values of 8.12 ± 0.05 nC, +63.7 ± 3.0 mV and 0.64 ± 0.01 were derived from the ON and OFF curves ($n = 5$). From Q_{max}, we derived the number (N) of cystinosin molecules expressed at the oocyte plasma membrane based on the identity:

$$N = Q_{max}/(z\delta^* q) \quad [2]$$

where q is the elementary charge. This yielded a mean number of approximately 8×10^{10} cystinosin molecules per oocyte in our conditions. Combined measurement of Q_{max} (at pH 7.5) and the steady-state current evoked by a saturating cystine concentration (at pH 5.0) showed that I_{max} is proportional to Q_{max}, with a

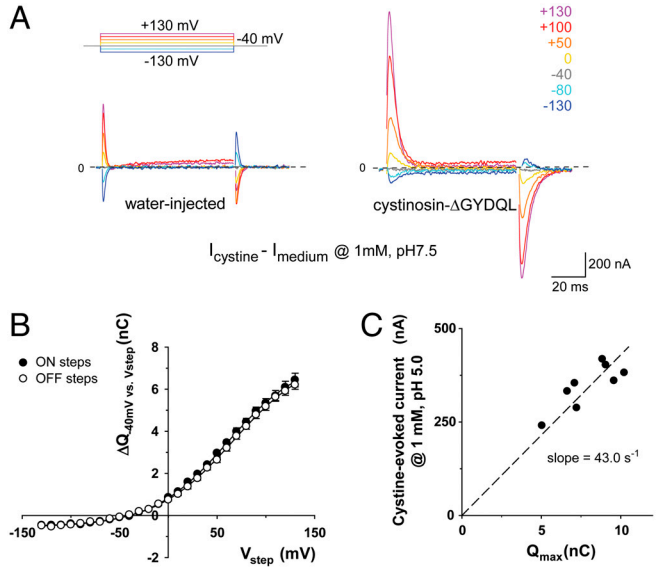

Fig. 4. Cystine-bound cystinosin shows transient capacitive currents. (*A*) Cystinosin-ΔGYDQL-EGFP oocytes held at −40 mV were stepped to various potentials (V_{step}) at pH_{out} 7.5, with or without cystine. Subtracted (cystine-dependent) traces are shown. In *B*, time integrals of the current peaks observed after the first (ΔQ_{ON}) and second (ΔQ_{OFF}) steps are plotted as a function of V_{step} (means ± s.e.m. of 5 oocytes with similar expression level). Curves were fitted with a Boltzmann distribution function. In C, the steady-state current elicited at pH_{out} 5.0 by 1 mM cystine is plotted against the amplitude of the Boltzmann function (Q_{max}) for 8 individual oocytes.

slope of 43 s^{-1} (Fig. 4*C*). From this value, we derived a transport cycle turnover (I_{max}/N) of 28 s^{-1} at pH 5.0.

Cystine-Dependent Charge Movements Are Carried by Extracellular Protons. We used two independent approaches to determine whether the charge movements reflect proton transfer events or electrogenic conformational changes. Firstly, we examined whether a change in pH_{out} shifts their midpoint voltage, $V_{0.5}$. This midpoint corresponds to the voltage at which the two states of the electrogenic transition are equally populated. If this transition is a protonation equilibrium, at $V_{0.5}$ the local pH around the protonatable site is equal to its pK_a (pK_{a2}, cystine-bound protein). Therefore, according to our model, $V_{0.5}$ should be related to the pK_{a2} and the fractional depth, δ, of the protonatable site relative to the extracellular compartment by the Woodhull equation:

$$pK_{a2} = pH_{out} + \frac{F\delta\, V_{0.5}}{2.3RT} \qquad [3]$$

A shift in pH_{out} should thus shift $V_{0.5}$ by:

$$\Delta V_{0.5} = -(2.3RT/\delta F)\Delta pH_{out} \approx -58.2\Delta pH_{out}/\delta \qquad [4]$$

The depth δ in Eq. **4** can be deduced from the elementary distance δ^* of the charge movement if we make an additional assumption on the valence, z, of the elementary charge moved. We previously determined that, regardless of the charge movement mechanism, $z\delta^* = 0.64$ (Fig. 4*B*). If the totality of the charge is carried by a single proton ($z = 1$) transferred from the extracellular medium to the buried site ($\delta^* = \delta$), δ would equal 0.64 and we would expect a decrease of $V_{0.5}$ by −90.9 mV when pH_{out} increases by 1 pH unit. If two protons are transferred through a fractional length $\delta^* = 0.32$, we would expect a $V_{0.5}$ shift of −182 mV. On the contrary, if the charge movement is predominantly carried by intrinsic charges of the protein rather than extracellular protons, $V_{0.5}$ should not depend on pH_{out} in a predictable manner.

To discriminate between these possibilities, we recorded cystine-dependent transient currents at both pH_{out} 7.5 and 8.5. Representative traces, representative Q-V_m relationships, and mean values of the Boltzmann distribution parameters are shown in Fig. 5 *A*, *B*, *E*, and *F*, respectively. Strikingly, not only did $V_{0.5}$ decrease at pH_{out} 8.5 (−29.3 ± 3.0 mV, $n = 8$ oocytes, ON steps) relative to pH_{out} 7.5 (66.7 ± 4.4 mV), as expected for a protonation equilibrium open to the extracellular medium, but the extent of the $\Delta V_{0.5}$ shift (−96.0 ± 7.4 mV) was consistent with our working model and the elementary transfer of one proton through 64% of the electric field (Fig. 5*F*). The transient current is thus carried by a single proton moving across the transmembrane electric field. This may occur either by physical transfer of the proton along a narrow (hence voltage-sensitive) access channel (34, 35) or by occlusion of the bound proton from the extracellular solution; in the latter case, the electric field moves across the fixed (bound) charge (36).

To confirm this conclusion and discriminate between the two structural models, we next examined whether the charge movements are slowed down in deuterated water. If the transient currents are carried by protons, substituting D_2O for H_2O should induce two effects. On one hand, the deuterium isotope effect should significantly increase their decay time; on the other hand, $V_{0.5}$ should be shifted rightward by approximately +50 mV because D_2O generally increases the pK_a of carboxylic acids by 0.5–0.6 units (37). We thus recorded cystinosin in standard water-based saline at pH 7.5 and in the corresponding heavy water solution at a pD(-log([D^+]) value of 7.5 (Fig. 5 *C* and *D*). In agreement with these predictions, we observed that D_2O induced a rightward shift of $V_{0.5}$ by +60.6 ± 13.2 mV (ON steps, $n = 8$; Fig. 5*F*) and increased decay times by an average factor of 1.93 ± 0.05 (ON steps, +20 to +130 mV range; Fig. 5*G*) relative to H_2O.

Taken together, these experiments are consistent with the view that the transient currents are carried by a dehydrated proton transferred from/to the extracellular compartment through a high-field access channel (proton wire) spanning 64% of the voltage gradient.

Noticeably, when protons are 10 times less abundant in the external solution (pH_{out} 8.5 vs. 7.5), transient currents were selectively slowed down at negative potentials (Fig. 5*G*)—i.e., when protons enter the access channel but not when they leave it, in good agreement with the access channel model. The modest imbalance between ON and OFF charges observed at negative potentials and pH_{out} 8.5 (Fig. 5 *B* and *E*) might originate from the existence of an additional, minor fast transient component that could not be properly separated from the oocyte membrane capacitance (thus escaping notice) at ON, but not OFF, steps. Quantitative analysis of the τ-V_m curves indicated that the energy barrier for proton transfer is located halfway along the access channel (see *SI Text*).

Neutralization-Scanning Mutagenesis Identifies D305 as the Proton Binding Site. We next performed a neutralization scan of protonatable residues to identify the proton binding site coupled to cystine binding. The scan was restricted to evolutionarily conserved residues, based on the fact that human cystinosin complements a yeast strain deleted for its putative orthologue Ers1 (21). Both strictly conserved residues and those changed to other protonatable amino acids across species were included, regardless of the predicted topology. This represents a set of 15 residues, which were individually changed to isosteric, nonprotonatable side chains. Fluorescence microscopy showed that none of the mutations prevented surface expression of cystinosin-ΔGYDQL-EGFP, thus allowing functional analysis. Four mutations strongly reduced (D161N) or abolished (D205N, D305N, K335Q) the steady-state current (Table S1). We then performed transient kinetic analysis to determine which protonatable residue(s) are

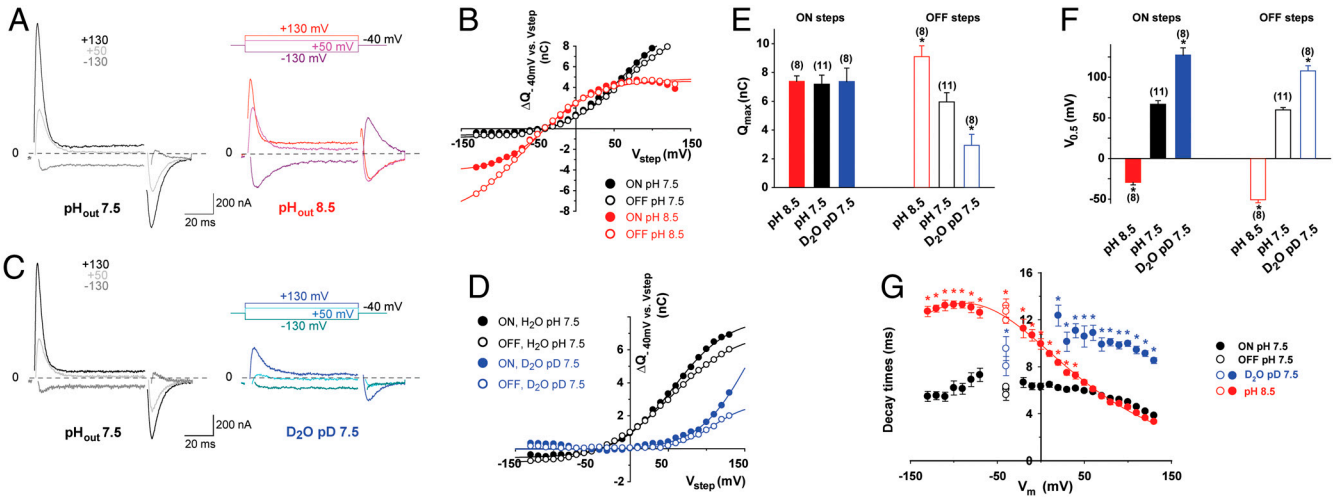

Fig. 5. Cystine-dependent transient currents are carried by extracellular protons. (*A* and *B*) An individual oocyte was stepped to various potentials successively at pH$_{out}$ 7.5 and pH$_{out}$ 8.5. Cystine-dependent traces and charge-voltage relationships are shown in *A* and *B*, respectively. (*C* and *D*) Another oocyte was analyzed similarly in standard medium at pH$_{out}$ 7.5 and in deuterated medium at pD$_{out}$ 7.5. (*E* and *F*) Maximal charges (Q_{max}) and midpoint voltages ($V_{0.5}$) for ON and OFF steps were determined (pH$_{out}$ 8.5, pH$_{out}$ 7.5) or extrapolated (pD$_{out}$ 7.5) by curve fitting. The extent of $V_{0.5}$ shift observed between pH$_{out}$ 8.5 and 7.5 is consistent with the transfer of one proton from the extracellular medium to a fractional membrane depth of 0.64. (*G*) Decay times are plotted against the membrane potential to which oocytes were stepped. For the OFF steps, 3 steps from −130, +50 and +130 mV to −40 mV are plotted. Transient currents are slowed in deuterated medium, and in aqueous pH$_{out}$ 8.5 medium when $V_m \leq +40$ mV. See also curve fitting analysis in *SI Text*. *$P < 0.05$ relative to pH$_{out}$ 7.5.

required for the charge movements. Several mutations affected their intrinsic properties by: decreasing the midpoint potential (Y281F, K335Q, D205N and, to a lesser extent, Y143F and D161N); altering the dielectric distance δ^* (Y143F, R152Q, K335Q); and slowing down (H211F) or accelerating (Y281F, K335Q) the time course (Fig. 6 *D* and *E* and Fig. S4). However, only one charge-neutralizing mutation, D305N, abolished the transient currents (Fig. 6 *B* and *C*), though the D305N protein was expressed at the plasma membrane (Fig. 6*B* and Fig. S1). The absolute, unique dependence of transient currents on D305, combined with the fact that they are carried by protons, strongly suggests that they reflect protonation/deprotonation of the D305 side chain.

Noticeably, the conservative mutation D305E also abolished transient currents at all membrane potentials tested (Fig. 6 *B* and *C* and Fig. S5), despite the modest pK_a shift (+0.4 units) theoretically induced by this mutation. Possible explanations

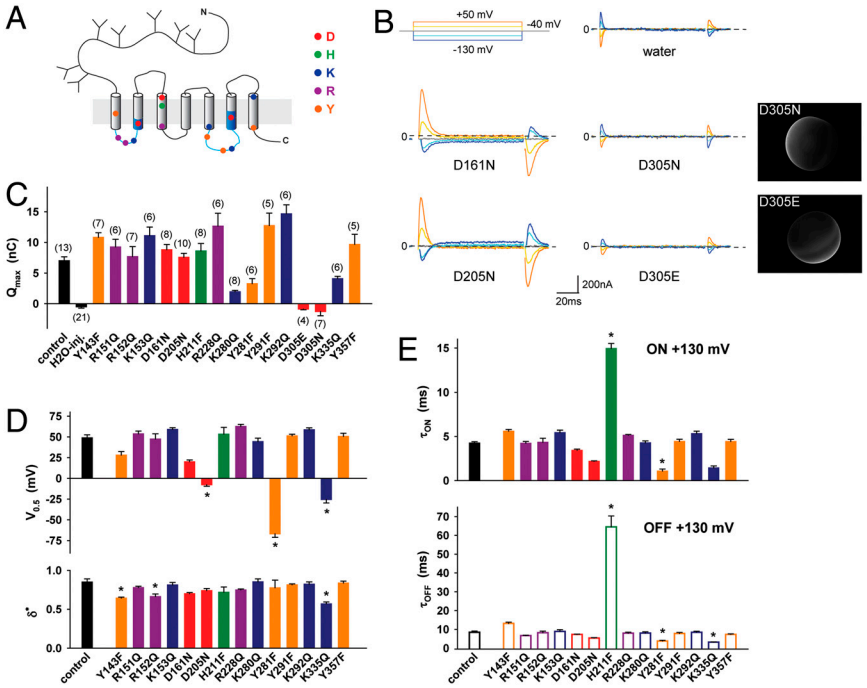

Fig. 6. D305 is uniquely required for the charge movements. (*A*) The relative position and nature of residues included in the neutralization scan is depicted on the topology model. These residues were individually mutated to isosteric, nonprotonatable amino acids and mutants were analyzed in voltage jumps experiments at pH$_{out}$ 7.5. (*B*) Representative traces of the aspartate mutants. Mutation of D305 to asparagine or glutamate abolished the transients. After recording, oocytes were disimpaled and observed by fluorescence microscopy to confirm surface expression of the D305 mutants. (*C* and *D*) Boltzmann distribution parameters were derived from ON-step Q-V_m curves. (*E*) Mean decay times of the transient currents caused by voltage steps to/from +130 mV. *$P < 0.05$ relative to the control construct.

could be that the larger glutamate side chain disrupts the proton wire or that its carboxyl group is locked in a protonated state because it reached a hydrophobic environment.

D305 Is Evolutionarily Conserved in a Subset of PQ-Loop Motifs. D305 is located within the second PQ motif of cystinosin (Fig. 1), yet it does not belong to the consensus sequence defining PQ loops (12, 23). We thus asked whether the presence of an acidic residue at this position has a broader significance among PQ-loop proteins. Among 893 PQ-loop motifs downloaded from the SMART database (38), 24% had an acidic residue at the position equivalent to D305 (Table 1). Among the 384 proteins harboring two PQ loops (like cystinosin) in this set, 46% had an acidic residue at the spotted position in one motif; however, none scored positively for both motifs. Intriguingly, while aspartate and glutamate residues had similar occurrences at protein level, a bias was observed in their distribution along the primary sequence: Whereas the N-terminal PQ loop showed a strong preference for glutamate over aspartate, the second PQ loop exclusively showed an aspartate (as in cystinosin) when an acidic residue was present at the spotted position (Table 1). Overall, our study and the fact that PQ-loop motifs are found in membrane proteins (Fig. S6) raise the possibility that other PQ-loop proteins may translocate protons. This could be the case of MPDU1, an endoplasmic reticulum protein defective in congenital disorders of glycosylation (39, 40) and required for utilization of mannose-P-dolichol (41), because it possesses a glutamate at the position equivalent to D305 in its first PQ loop.

Discussion

In this study, we show that human cystinosin operates as a 1:1 proton/cystine symporter; we identify a proton binding site cooperatively coupled to cystine binding; and we show that this proton binding site is nested within a PQ-loop motif and buried in the membrane, yet open to the lysosomal lumen probably through a proton wire.

Properties of the Binding Site for Luminal Protons The location of the proton binding site in the transmembrane electric field is supported by the fact that hyperpolarization could compensate for an increase in pH_{out} in both K_m-V_m and Q-V_m relationships. Similar relationships between the driving ion concentration and membrane voltage have been previously reported for other transporters (32, 33, 42–44). As mentioned above, the driving ion may sense the voltage drop either because it migrates along an access channel (35) or because it is occluded after binding (45). The latter mechanism is supported by structural studies in several secondary active transporters (see ref. 46 for review), whereas the former is well documented in P-type ATPases (4, 47–50), rotary ATPases (51), bacteriorhodopsins (13) and ClC chloride transport proteins (52). Although we cannot totally exclude an ion occlusion mechanism for cystinosin, our deuterium isotope substitution experiments apparently favor the access channel model. The approximately twofold kinetic effect observed in cystinosin, which is identical to the conductance decrease of voltage-gated proton channels in D_2O (37), is consistent with the transfer of naked protons along hydrogen-bonded chains (proton "wire").

It may be objected that the kinetics of the transient currents (100 to 250 s^{-1} at pH_{out} 7.5) is orders of magnitude slower than that of typical ion channels (10^6–10^7 s^{-1}). However, such a comparison would be misleading because the concentration of the permeating species is much lower with protons (3.10^{-9} to 10^{-5} M in our study) than other ions. When compared to proton channels, the access channel of cystinosin is in fact as fast as gramicidin (approximately 100 $H^+ s^{-1}$ at pH 7 and 100 mV) and only approximately 30-fold slower than voltage-gated and F_0 proton channels (3,000 to 6,000 $H^+ s^{-1}$) (53–56) (see also *SI Text*). Interestingly, proton transfer was strongly slowed down (four- to eightfold depending on the voltage jump) after neutralizing H211 (Fig. 6*E*), thus suggesting that this residue might participate in the proton wire.

Another significant feature of the proton binding site is its dielectric depth in the membrane, as it is separated from the lysosomal lumen by approximately 65% of the membrane electric field. This suggests that D305 acts as a relay site for proton translocation rather than as an allosteric regulatory site. The luminal proton bound to D305 may thus be released to the cytosolic side at subsequent steps of the transport cycle. However, it should be noted that protonation of D305 is not sufficient to complete the transport cycle since steady-state current remained low at $pH_{out} \geq 7.0$ when the membrane was hyperpolarized. Another luminal proton should thus bind elsewhere, possibly to D205 or D161, in a voltage-independent manner to promote continuing transport. This second luminal proton may regulate the conformational change of the loaded transporter to a cytosol-facing state; help D305 release its proton to the cytosolic side; or promote the backward conformational change of the empty transporter.

Cystine Binding Presumably Shifts the pK_a of D305. The cooperativity between proton and cystine binding is supported by two pieces of evidence: (*i*) pH_{out} or voltage conditions that favor protonation increase the apparent affinity for cystine (Fig. 3*C*) and, conversely, (*ii*) cystinosin binds luminal protons (through an electrogenic process) in the presence of cystine (Fig. 5). The strict and unique dependence of the latter process on the presence of an aspartate at position 305 strongly suggests that its side chain is the proton acceptor. In agreement with this crucial role, mutation of this residue to glycine or tyrosine causes infantile cystinosis (27, 28).

Which mechanism underlies this cooperativity? An answer can be inferred if we compare the effective pK_a derived from steady-state and transient current analyses. Application of Eq. **3** to $V_{0.5}$ values obtained at pH_{out} 7.5 or 8.5 yields a pK_{a2} of 8.2 for the cystine-bound state. Similarly, a pK_{a2} of 7.9 can be derived from the τ-V_m curves (see *SI Text*). On the other hand, a kinetic model of the K_m-V_m curves yields an effective pK_{a1} of 6.3 for the cystine-free state of cystinosin (see *SI Text*), thus suggesting that cystine binding might promote proton binding by increasing the pK_a of D305 by approximately 2 pH units. As our model was deliberately simplified and blind to states with an inward-facing (toward the cytoplasm) substrate-binding site, this tentative conclusion should be directly tested in the future using voltage jump experiments in the absence of cystine.

In evolutionarily divergent proton pumps, a membrane-buried aspartate acts as a central proton relay site accessible through proton channels and proton loading/unloading throughout the pumping cycle is ensured by pK_a shifts caused by movements of a nearby positively charged residue—see ref. 57 for review. Future studies may explore whether cystinosin handles luminal protons in an analogous way and may identify side chains stabilizing the protonated and deprotonated states of D305. Notice-

Table 1. Evolutionary conservation of D305 in PQ-loop motifs

Type of PQ-loop motif	Number of occurrences at position equivalent to D305			
	any amino acid	D	E	D or E
Single PQ loop	125	5	33	38
First motif of pair	384	8	69	77
Second motif of pair	384	98	0	98
Both motifs of pair	384	0	0	0

PQ-loop sequences from 509 proteins found in diverse eukaryotes were downloaded from the SMART database (entry SM00679) and analyzed for the presence of an acidic residue at position +21 downstream the canonical PQ dipeptide.

ably, mutation Y281F decreased $V_{0.5}$ by −110 mV (Fig. 6*D*). This shift would correspond to a 1.2-unit decrease in the pK_{a2} of D305, raising the possibility that Y281 might be a hydrogen bond acceptor stabilizing the protonated state of D305. However, Y281F might also act through indirect structural alterations, as highlighted by the existence of several mutations with similar, yet lesser, effect scattered along the primary sequence. Structural approaches are needed to discriminate these possibilities.

Material and Methods

Expression of Human Cystinosin in *Xenopus* Oocytes. Experiments were performed in agreement with local and national guidelines for use of animals and their care. Ovarian lobes were extracted from *Xenopus laevis* females under anesthesia and oocyte clusters were incubated on a shaker in OR2 medium (85 mM NaCl, $MgCl_2$ 1 mM, 5 mM Hepes-K^+ pH 7.6) containing 2 mg/mL of collagenase type II (GIBCO) for 1 h at room temperature. Defolliculated oocytes were sorted and kept at 19 °C in Barth's solution (88 mM NaCl, 1 mM KCl, 2.4 mM $NaHCO_3$, 0.82 mM $MgSO_4$, 0.33 mM $Ca(NO_3)_2$, 0.41 mM $CaCl_2$, 10 mM Hepes-Na^+ pH 7.4), supplemented with 50 μg/mL of gentamycin.

Capped cRNAs were synthesized in vitro from linearized pCRII and pOX(+) plasmids (see *SI Methods*) using mMessage-mMachine T7 and SP6 kits (Ambion), respectively. Oocytes were injected with 50 ng of cRNA using a nanoliter injector (World Precision Instruments). Expression of EGFP-tagged constructs at the oocyte surface was verified under an Eclipse TE-2000 epifluorescence microscope (Nikon) with a 4x objective lens and used to preselect oocytes with highest expression levels for electrophysiological recording. Epifluorescence micrographs were acquired with a CCD camera (Coolsnap) and processed using ImageJ.

Voltage-Clamp Analysis. Electrophysiological recording was performed at room temperature usually two days after cRNA injection. Voltage clamp was applied using an OpusXpress 6000A workstation (Molecular Devices) or a rapid perfusion setup with an O725C amplifier (Warner Instrument) and two borosilicate-glass microelectrodes filled with 3 M KCl (0.3–2 MΩ tip resistance) and an Ag/AgCl reference electrode located close to the oocyte. Currents were recorded using a Digidata 1320 interface and the pClamp software (Molecular Devices).

Oocytes were perfused with ND100 solutions (100 mM NaCl, 2 mM KCl, 1 mM $MgCl_2$, 1.8 mM $CaCl_2$, 5 mM HEPES or MES adjusted to the required pH with CsOH) supplemented, or not, with L-cystine or other compounds (all from Sigma). For isotope effect experiments, we used 99.8% deuterium oxide (Euriso-Top) as a solvent and adjusted the pD of the ND100 solution with CsOH by adding a correction of 0.40 units to the nominal reading of the pH meter (37).

Steady-state currents were generally recorded using the automated OpusXpress 6000A workstation and robotic compound delivery from 96-well plates. Current traces acquired at a constant holding potential (−40 mV) were filtered at 5 Hz and sampled at 500 Hz. Blank application of ND100 buffer from the OpusXpress liquid handler generated a small outward-current artefact that was subtracted from cystine-evoked currents in subsequent data analysis. To characterize the voltage dependence of steady-state currents, traces were filtered at 500 Hz and sampled at 6.25 kHz, and voltage steps were applied from +20 mV to −100 mV with −10 mV increments. Saturation kinetics of control cystinosin-ΔGYDQL were analyzed using eight cystine concentrations ranging from 7.8 μM to 1 mM, the maximal achievable concentration at pH ≥ 5.0. For practical reasons, this range was narrowed to 32 μM-1 mM when this analysis was repeated on the various point mutants of this study.

Transient currents were recorded on the conventional setup using a tubular perfusion chamber that allows a fast, laminar flow around the oocyte. The perfused solution was changed manually by means of a motorized valve. Currents were filtered at 1 kHz and digitized at 50 kHz. Oocytes previously equilibrated in the ND100 buffer at pH 7.5 or 8.5 without cystine were held at −40 mV and stepped from +130 mV to −130 mV with −10 mV increments. Steps were repeated after cystine (1 mM) was applied at the same pH for approximately 20 s and, subsequently, after a 1-min wash to check the stability of current traces. Water-injected oocytes showed small, fast, symmetrical cystine-dependent transients, which varied in magnitude and direction among experiments (compare Figs. 4*A* and 6*B*). These variations presumably reflect minor changes in the oocyte passive capacitance caused by slight pH differences (≤0.02 Units) between the cystine-containing and cystine-free media.

Current traces were analyzed offline using the Clampfit 9 software (Molecular Devices). Graphs and nonlinear regressions were performed using SigmaPlot (Systat Software). Results are expressed as mean ± s.e.m, with the number of oocytes indicated in parentheses. Statistical analysis was performed using one-way analysis of variance (ANOVA) followed by the post hoc Dunnett's test, or Kruskal-Wallis nonparametric one-way ANOVA with post hoc Dunn's test, as appropriate.

Cystine Uptake Under Voltage Clamp. L-[^{35}S]cystine (Perkin-Elmer) solutions were applied to oocytes under two-electrode voltage-clamp on the conventional setup. After recording, electrodes were disimpaled, oocytes were briefly washed in chilled buffer and the accumulated radioactivity was counted in Emulsifier-Safe cocktail (Packard) using a Tri-Carb 2100 TR liquid scintillation analyzer (Packard). Cystine concentrations (8 μM to 1 mM), the pH of ND100 solution (5.0 to 6.5) and holding potentials (−20 to −80 mV) were varied to obtain a wide range of cystine uptake values.

Extracellular pH Recording. Extracellular pH measurements were performed as previously (58). Briefly, H^+-selective microelectrodes, previously silanized with dichlorodimethylsilane (Sigma), backfilled with the proton ionophore B (Fluka) and filled with 150 mM NaCl, 23 mM NaOH, 40 mM KH_2PO_4, pH 6.8, were placed close to the voltage-clamped oocyte at a holding potential of +20 mV or −80 mV. Cystine-evoked currents and local extracellular pH variations were simultaneously measured using external bath solutions buffered with 0.2 mM MES at pH 5.0 or 6.0. (See also *SI Methods*.)

ACKNOWLEDGMENTS. We thank H. Daniel and M. Hediger for reagents; B. Langen for help in some experiments; S. Birman, J. P. Henry, and M. Le Maire for comments on the manuscript. This study was supported by the Centre National de la Recherche Scientifique, the Cystinosis Research Foundation (grant to B.G.), the Consiglio Nazionale delle Ricerche, Telethon Italy (Grant GGP08064 to M.P.), and the Italian Institute of Technology (grant SEED to M.P.). R.R. was supported by a fellowship from the Portuguese Fundação para a Ciência e a Tecnologia. X.C. is supported by the Cystinosis Research Foundation. C.S. and S.S. are scientists from the Institut National de la Santé et de la Recherche Médicale.

1. Miller C (2006) ClC chloride channels viewed through a transporter lens. *Nature* 440:484–489.
2. Pusch M, Jentsch TJ (2005) Unique structure and function of chloride transporting CLC proteins. *IEEE Trans Nanobioscience* 4:49–57.
3. Gadsby DC, Takeuchi A, Artigas P, Reyes N (2009) Review. Peering into an ATPase ion pump with single-channel recordings. *Philos Trans R Soc Lond B Biol Sci* 364:229–238.
4. Takeuchi A, Reyes N, Artigas P, Gadsby DC (2008) The ion pathway through the opened Na^+, K^+-ATPase pump. *Nature* 456:413–416.
5. Feng L, Campbell EB, Hsiung Y, MacKinnon R (2010) Structure of a eukaryotic CLC transporter defines an intermediate state in the transport cycle. *Science* 330:635–641.
6. Jayaram H, Accardi A, Wu F, Williams C, Miller C (2008) Ion permeation through a Cl—selective channel designed from a CLC Cl^-/H^+ exchanger. *Proc Natl Acad Sci USA* 105:11194–11199.

7. Lisal J, Maduke M (2008) The ClC-0 chloride channel is a 'broken' Cl^-/H^+ antiporter. *Nat Struct Mol Biol* 15:805–810.
8. Zdebik AA, et al. (2008) Determinants of anion-proton coupling in mammalian endosomal CLC proteins. *J Biol Chem* 283:4219–4227.
9. Gadsby DC (2009) Ion channels versus ion pumps: The principal difference, in principle. *Nat Rev Mol Cell Biol* 10:344–352.
10. Town M, et al. (1998) A novel gene encoding an integral membrane protein is mutated in nephropathic cystinosis. *Nat Genet* 18:319–324.
11. Kalatzis V, Cherqui S, Antignac C, Gasnier B (2001) Cystinosin, the protein defective in cystinosis, is a H^+-driven lysosomal cystine transporter. *EMBO J* 20:5940–5949.
12. Zhai Y, Heijne WH, Smith DW, Saier MH, Jr (2001) Homologues of archaeal rhodopsins in plants, animals and fungi: structural and functional predications for a putative fungal chaperone protein. *Biochim Biophys Acta* 1511:206–223.
13. Lanyi JK (2006) Proton transfers in the bacteriorhodopsin photocycle. *Biochim Biophys Acta* 1757:1012–1018.
14. Spudich JL, Yang CS, Jung KH, Spudich EN (2000) Retinylidene proteins: Structures and functions from archaea to humans. *Annu Rev Cell Dev Biol* 16:365–392.
15. Waschuk SA, Bezerra AG, Jr, Shi L, Brown LS (2005) Leptosphaeria rhodopsin: Bacteriorhodopsin-like proton pump from a eukaryote. *Proc Natl Acad Sci USA* 102:6879–6883.
16. Balashov SP, et al. (2005) Xanthorhodopsin: A proton pump with a light-harvesting carotenoid antenna. *Science* 309:2061–2064.
17. Gahl WA, Bashan N, Tietze F, Bernardini I, Schulman JD (1982) Cystine transport is defective in isolated leukocyte lysosomes from patients with cystinosis. *Science* 217:1263–1265.
18. Jonas AJ, Smith ML, Schneider JA (1982) ATP-dependent lysosomal cystine efflux is defective in cystinosis. *J Biol Chem* 257:13185–13188.
19. Gahl WA, Thoene JG, Schneider JA (2002) Cystinosis. *N Engl J Med* 347:111–121.
20. Kalatzis V, Antignac C (2003) New aspects of the pathogenesis of cystinosis. *Pediatr Nephrol* 18:207–215.
21. Gao XD, Wang J, Keppler-Ross S, Dean N (2005) ERS1 encodes a functional homologue of the human lysosomal cystine transporter. *Febs J* 272:2497–2511.
22. Cherqui S, Kalatzis V, Trugnan G, Antignac C (2001) The targeting of cystinosin to the lysosomal membrane requires a tyrosine-based signal and a novel sorting motif. *J Biol Chem* 276:13314–13321.
23. Ponting CP, Mott R, Bork P, Copley RR (2001) Novel protein domains and repeats in Drosophila melanogaster: Insights into structure, function, and evolution. *Genome Res* 11:1996–2008.
24. Chaudhry FA, et al. (2001) Coupled and uncoupled proton movement by amino acid transport system N. *EMBO J* 20:7041–7051.
25. Borre L, Kavanaugh MP, Kanner BI (2002) Dynamic equilibrium between coupled and uncoupled modes of a neuronal glutamate transporter. *J Biol Chem* 277:13501–13507.
26. Fairman WA, Vandenberg RJ, Arriza JL, Kavanaugh MP, Amara SG (1995) An excitatory amino-acid transporter with properties of a ligand-gated chloride channel. *Nature* 375:599–603.
27. Attard M, et al. (1999) Severity of phenotype in cystinosis varies with mutations in the CTNS gene: Predicted effect on the model of cystinosin. *Hum Mol Genet* 8:2507–2514.
28. Shotelersuk V, et al. (1998) CTNS mutations in an American-based population of cystinosis patients. *Am J Hum Genet* 63:1352–1362.
29. Greene AA, Marcusson EG, Morell GP, Schneider JA (1990) Characterization of the lysosomal cystine transport system in mouse L-929 fibroblasts. *J Biol Chem* 265:9888–9895.
30. Sagné C, Gasnier B (2008) Molecular physiology and pathophysiology of lysosomal membrane transporters. *J Inherit Metab Dis* 31:258–266.
31. Woodhull AM (1973) Ionic blockage of sodium channels in nerve. *J Gen Physiol* 61:687–708.
32. Mager S, et al. (1993) Steady states, charge movements, and rates for a cloned GABA transporter expressed in Xenopus oocytes. *Neuron* 10:177–188.
33. Parent L, Supplisson S, Loo DD, Wright EM (1992) Electrogenic properties of the cloned Na^+/glucose cotransporter: I Voltage-clamp studies. *J Membr Biol* 125:49–62.
34. Mitchell P (1968) *Chemiosmotic Coupling and Energy Transduction* (Glynn Research, Bodmin, UK).
35. Läuger P (1991) *Electrogenic Ion Pumps* (Sinauer Associates, Sunderland MA).
36. Hilgemann DW, Lu CC (1999) GAT1 (GABA:Na^+:Cl^-) cotransport function database reconstruction with an alternating access model. *J Gen Physiol* 114:459–475.
37. DeCoursey TE, Cherny VV (1997) Deuterium isotope effects on permeation and gating of proton channels in rat alveolar epithelium. *J Gen Physiol* 109:415–434.
38. Schultz J, Milpetz F, Bork P, Ponting CP (1998) SMART, a simple modular architecture research tool: identification of signaling domains. *Proc Natl Acad Sci USA* 95:5857–5864.
39. Schenk B, et al. (2001) MPDU1 mutations underlie a novel human congenital disorder of glycosylation, designated type If. *J Clin Invest* 108:1687–1695.
40. Kranz C, et al. (2001) A mutation in the human MPDU1 gene causes congenital disorder of glycosylation type If (CDG-If). *J Clin Invest* 108:1613–1619.
41. Ware FE, Lehrman MA (1996) Expression cloning of a novel suppressor of the Lec15 and Lec35 glycosylation mutations of Chinese hamster ovary cells. *J Biol Chem* 271:13935–13938.
42. Forster I, Hernando N, Biber J, Murer H (1998) The voltage dependence of a cloned mammalian renal type II Na^+/Pi cotransporter (NaPi-2). *J Gen Physiol* 112:1–18.
43. Jauch P, Läuger P (1986) Electrogenic properties of the sodium-alanine cotransporter in pancreatic acinar cells: II Comparison with transport models. *J Membr Biol* 94:117–127.
44. Wadiche JI, Arriza JL, Amara SG, Kavanaugh MP (1995) Kinetics of a human glutamate transporter. *Neuron* 14:1019–1027.
45. Lu CC, Hilgemann DW (1999) GAT1 (GABA:Na^+:Cl^-) cotransport function Kinetic studies in giant Xenopus oocyte membrane patches.. *J Gen Physiol* 114:445–457.
46. Krishnamurthy H, Piscitelli CL, Gouaux E (2009) Unlocking the molecular secrets of sodium-coupled transporters. *Nature* 459:347–355.
47. Nakao M, Gadsby DC (1986) Voltage dependence of Na translocation by the Na/K pump. *Nature* 323:628–630.
48. Olesen C, et al. (2007) The structural basis of calcium transport by the calcium pump. *Nature* 450:1036–1042.
49. Poulsen H, et al. (2010) Neurological disease mutations compromise a C-terminal ion pathway in the Na^+/K^+-ATPase. *Nature* 467:99–102.
50. Reyes N, Gadsby DC (2006) Ion permeation through the Na^+,K^+-ATPase. *Nature* 443:470–474.
51. Junge W, Sielaff H, Engelbrecht S (2009) Torque generation and elastic power transmission in the rotary F(O)F(1)-ATPase. *Nature* 459:364–370.
52. Zifarelli G, Pusch M (2010) The role of protons in fast and slow gating of the Torpedo chloride channel ClC-0. *Eur Biophys J* 39:869–875.
53. Cherny VV, Murphy R, Sokolov V, Levis RA, DeCoursey TE (2003) Properties of single voltage-gated proton channels in human eosinophils estimated by noise analysis and by direct measurement. *J Gen Physiol* 121:615–628.
54. Cukierman S, Quigley EP, Crumrine DS (1997) Proton conduction in gramicidin A and in its dioxolane-linked dimer in different lipid bilayers. *Biophys J* 73:2489–2502.
55. Feniouk BA, et al. (2004) The of ATP synthase: Ohmic conductance (10 fS), and absence of voltage gating. *Biophys J* 86:4094–4109.
56. Franklin MJ, Brusilow WSA, Woodbury DJ (2004) Determination of proton flux and conductance at pH 6 8 through single Fo sectors from *Escherichia coli. Biophys J* 87:3594–3599.
57. Buch-Pedersen MJ, Pedersen BP, Veierskov B, Nissen P, Palmgren MG (2009) Protons and how they are transported by proton pumps. *Pflugers Arch* 457:573–579.
58. Picollo A, Pusch M (2005) Chloride/proton antiporter activity of mammalian CLC proteins ClC-4 and ClC-5. *Nature* 436:420–423.